Molecular Dynamics Simulations of Six Different Fully Hydrated Monomeric Conformers of *Escherichia coli* Re-Lipopolysaccharide in the Presence and Absence of Ca^{2+}

Stefan Obst, Manfred Kastowsky, and Hans Bradaczek
Freie Universität Berlin, Institut für Kristallographie, D-14195 Berlin, Germany

ABSTRACT Six previously published conformational models of *Escherichia coli* Re lipopolysaccharide (ReLPS) were subjected to molecular dynamics simulations using the CHARMM force field. The monomers of ReLPS were completely immersed in a water box. The dynamic behavior of the solvated models in the presence and absence of calcium cations was compared. The structure of the solvent shell was analyzed in terms of radial distribution functions. Diffusion coefficients and mean residence times were analyzed to characterize the dynamic behavior of the solvent. Order parameters and number of *gauche* defects were used for the description of the dynamics of the acyl chains. The cations are preferentially located between the carboxylate and phosphate groups of the headgroup. Their presence leads to a rigidification of the headgroup structure and alters the conformation of the backbone, thus influencing the structure and flexibility of the hydrophobic region as well. The effect of calcium on the backbone flexibility was measured in terms of glycosidic torsion angles. The six fatty acid chains of each ReLPS monomer adopt a highly ordered micromembrane structure. The packing parameter indicates that aggregation of these ReLPS monomers will lead to lamellar structures. Evaluation of all data enables us to present one conformation, C, which is thought to best represent the average structure of the ReLPS conformers.

INTRODUCTION

Bacterial lipopolysaccharides (LPS) are the major constituents of the outer leaflet of the outer membrane of Gram-negative bacteria (Nikaido and Vaara, 1987; Helander et al., 1995). Moreover, they are potent stimulators of the immune system (Doran, 1992; Martich et al., 1993). So-called septic shock is the most severe outcome of an exposure to endotoxins and results in the death of 25% of 400,000 patients showing symptoms of septic shock in the United States each year (Centers for Disease Control, 1990). Therefore, LPS have been the subject of intense study over the past 30 years (Rietschel and Brade, 1992).

The chemical structure of a large number of LPS of different species has been determined (Rietschel et al., 1994). Basically, LPS consists of a lipid portion, termed lipid A, which is the endotoxic principal of LPS (Brade et al., 1988; Rietschel et al., 1993; Zähringer et al., 1994), and a polysaccharide part, which is specific to the bacterial species (Raetz, 1990; Zähringer et al., 1994). Typically, lipid A consists of a β-1,6-diglucosamine backbone carrying six fatty acid chains, two phosphate groups, and the polysaccharide part. The latter can be divided into core and *o*-antigen regions. In the inner core, characteristic sugars like 2-keto-3-deoxyoctolusonic acid (KDO) can be found, whereas outer core and *o*-antigen contain mainly hexoses (Zähringer et al., 1994). Recently it was shown that the structure of the disaccharide backbone is essential for the binding of lipid A to cells and that the structure of the hydrophobic part influences the ability to induce cytokine production in cells (Kirikae et al., 1994). The LPS investigated in the present study is termed ReLPS and consists of the lipid A portion and a dimer of KDO (Zähringer et al., 1985; Imoto et al., 1985a,b). It represents the smallest LPS structure found in viable *Escherichia coli* bacteria (Rietschel et al., 1984; Raetz et al., 1991).

Although much is known about the chemical composition of LPS, the three-dimensional structure remains to be investigated. Crystals of *Salmonella* LPS exist (Kato et al., 1993), but to our knowledge, a single crystal x-ray analysis at atomic resolution has not been carried out successfully until now. Recently the aggregation of LPS has been studied by Monte Carlo methods, using simple geometric structures like triangles and rods for the representation of the LPS (Jung and Hollingsworth, 1996). On the atomic level, structural models of LPS have been proposed by Kastowsky et al. that are based on Monte Carlo calculations supported by x-ray investigations of LB films and Fourier transform infrared and neutron scattering data (Labischinski et al., 1985; Kastowsky et al., 1991b, 1992, 1993; Kastowsky, 1993; Seydel et al., 1993).

In 1991, six equivalent models of ReLPS of *E. coli* were published (Kastowsky et al., 1991b). Because no further discrimination between these models was possible on the basis of the Monte Carlo method, which basically gives a static snapshot of a molecule, we decided to use molecular dynamics (MD) simulations (van Gunsteren and Berendsen, 1990; Karplus and Petsko, 1990) to assess the dynamic behavior of these models.

Received for publication 29 April 1996 and in final form 9 December 1996.

Address reprint requests to Dr. Stefan Obst, Institut für Kristallographie, Freie Universität Berlin, Takustrasse 6, D-14195, Berlin, Germany. Tel.: 49-30-838-3457; Fax: 49-30-838-3464; E-mail: obst@chemie.fu-berlin.de.

Dr. Kastowsky's present address is William S. Middleton Memorial VA Hospital, Mycobacterial Research Lab., 2500 Overlook Terrace, Madison, WI 53705.

0006-3495/97/03/1031/16 $2.00

In the present work we investigated monomers of ReLPS, which were completely immersed in a box of water. For each of the six conformational models MD simulations were carried out in the presence and absence of calcium ions.

In the following we will give our reasons for using this setup. We concentrated on monomers of ReLPS for two reasons.

First, strong evidence suggests that the biologically active form of ReLPS is the monomer. In recent years, a number of proteins were isolated and identified that are capable of binding LPS at a varying degree of specificity. Hemoglobin (Kaca et al., 1994) and albumin (David et al., 1995b) are two of the less specific LPS-binding proteins. More specific interactions were found between LPS and BPI (Gray et al., 1989), LBP (Tobias et al., 1989; Schumann et al., 1990), CD14 (Wright et al., 1990), and antibodies (Appelmelk et al., 1995). Whereas a less specific interaction might be possible with aggregates of LPS, the specific interaction, especially between antibodies and epitopes that are buried in aggregates, might require monomeric LPS (Morrison, 1989). The question of the influence of the aggregation state of the LPS on its biological activity has been discussed controversially in the past (Shnyra et al., 1993; Takayama et al., 1994). Undoubtedly amphiphilic LPS generally has a tendency to adopt multimeric aggregate structures like the lamellar aggregates in the bacterial membrane (Seydel et al., 1993; Shnyra et al. 1993). On the other hand, the LPS-receptor interaction presumably is a monomer-receptor interaction (Morrison, 1989), and indeed a small amount of monomeric LPS (<1%) is found in LPS preparations, as demonstrated by Takayama et al. (1990).

Moreover, it was shown that isolated, highly dispersed LPS, shed by bacteria (Risco and Pinto da Silva, 1995) or released by lysis, is more active in the standard assay for endotoxin measurements, the chromogenic *Limulus* amebocyte lysate assay (CLAL), than LPS that is tightly packed in the bacterial outer membrane (Mattsby-Baltzer et al., 1991). The LPS-BPI interaction is increased for isolated LPS as compared to the interaction with complete bacteria (Capodici et al., 1994). Finally, Takayama et al. demonstrated that the monomeric form is the biologically active form of LPS (Takayama et al., 1990, 1994; Din et al., 1993). Monomeric LPS is 179-fold more active in the CLAL assay and 1000-fold more active in Egr-1 mRNA induction than aggregates of LPS (Takayama et al., 1994).

The second reason for investigating monomers was that we wanted to understand the behavior of the monomer before trying to simulate the far more complex aggregates. Moreover, using a single molecule prevents us from confusing molecular effects with aggregate effects, which result from the supramolecular assembly (Brandenburg et al., 1993).

Investigation of six different models at the same time enabled us to cover a greater part of the conformational space available to these molecules than would have been possible if only one model had been used for a longer simulation.

By comparison of simulations carried out in the presence and absence of calcium cations for each ReLPS conformation, we were able to investigate the influence of these bivalent ions on the structure and the dynamic behavior of the ReLPS molecules. Bivalent cations, especially magnesium and calcium, are known to be associated with LPS and are essential for the structure and function of the bacterial outer membrane (Coughlin et al., 1983a,b; Vaara, 1992; Pelletier et al., 1994).

MATERIALS AND METHODS

The atomic coordinates of the ReLPS models were those published by Kastowsky et al. (1991b) (cf. Fig. 1), and the numbering of the structures (A-F) follows figure 8 of that publication. The suffix -Ca indicates the presence of two calcium ions during the simulation. In Fig. 2 the chemical structure of this *E. coli* ReLPS (Zähringer et al., 1985) is shown.

Charges were calculated using the CNDO method (Gutberlet, 1989). The ionization state was set according to calculations of Takayama (Din et al., 1993), yielding four negative charges per monomer at physiological pH. Negative charges are located at the two phosphate groups and at the carboxylate groups of the KDOs. The molecular dynamics calculations were carried out using the CHARMM force field (Brooks et al., 1983) V.22 as supplied by MSI (Molecular Simulations, Waltham, MA). The structures were subjected to energy minimization using the steepest descent (SD) and Adopted Basis Newton-Raphson (ABNR) algorithms.

In the following, a typical setup used for the simulations is described. The position of the calcium ions was determined in vacuo using a grid search algorithm with a step width of 1 Å. A Ca^{2+} ion was placed on a virtual grid in the vicinity of the ReLPS molecule. The energy was minimized by 50 steps of SD minimization while keeping the coordinates of the ReLPS molecule fixed. The resulting energy was saved, together with the coordinates. After evaluation of the entire grid, which comprised

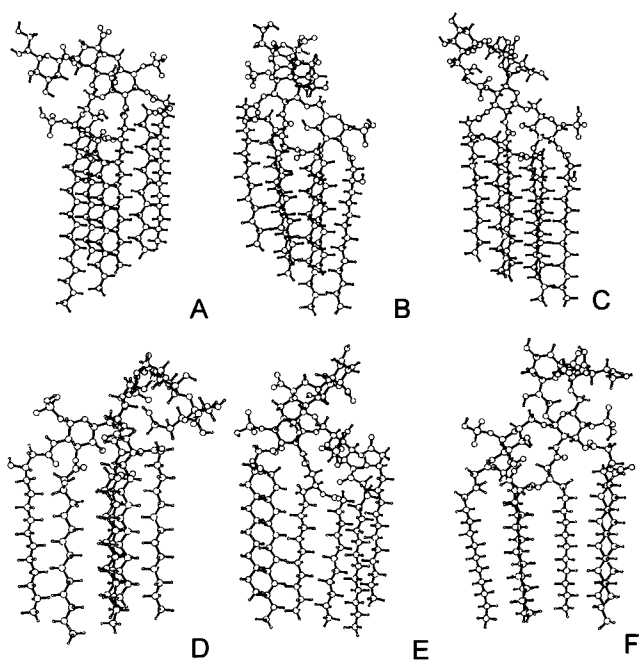

FIGURE 1 Six starting conformations of ReLPS (cf. figure 8 in Kastowsky et al., 1991b). The conformers are named according to the original paper. Ball-and-stick models were generated using SCHAKAL (E. Keller, Freiburg, Germany).

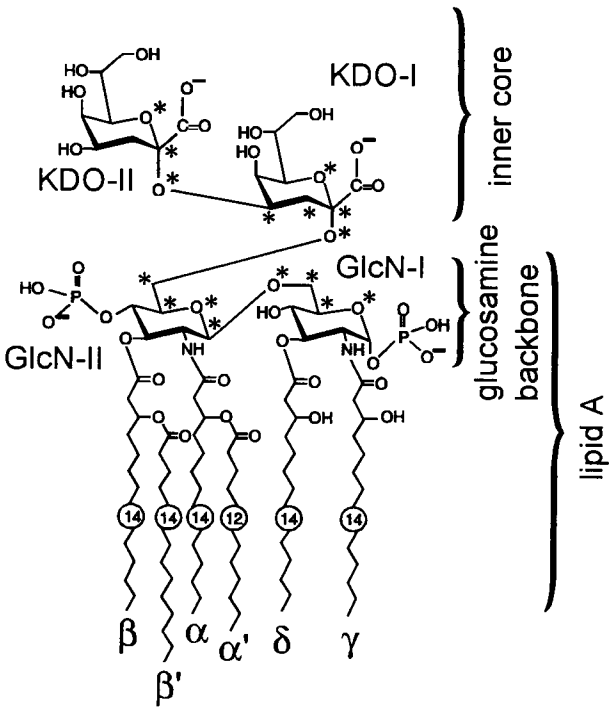

FIGURE 2 The chemical structure of ReLPS of *E. coli*, which consists of a lipid A part and an inner core region (Zähringer et al., 1985). The core is represented by an α-(2,4)-dimer of 2-keto-3-deoxyoctolusonic acid (KDO). The core is connected to the lipid A by an α-(2,6) glycosidic bond. The lipid A moiety consists of a β-D-glucosaminyl-(1,6)-β-D-glucosamine with two phosphoryl groups attached to position 1 of the reducing (GlcN-I) and to position 4′ of the nonreducing (GlcN-II) glucosaminyl residue. Four chains of (*R*)-3-hydroxytetradecanoic acid are linked by amide and ester bonds to the 2 and 2′ and the 3 and 3′ positions of the glucosamine backbone, respectively. The hydroxy acid chains in the 2′ and 3′ positions are acylated with a dodecanoic and a tetradecanoic acid chain, respectively. Acyl chains are labeled by Greek characters. Headgroup atoms involved in glycosidic torsions are marked by asterisks.

up to 16,000 points, the saved structures were clustered and the representatives of the 20 lowest energy structures were minimized again, using 500 steps of SD minimization. The resulting structure with the lowest energy was chosen to give the position of the first Ca^{2+} ion. This procedure was repeated during the determination of the best position of the second Ca^{2+} cation while fixing the first cation in its previously obtained position.

The ReLPS monomer was completely immersed in a rectangular box of preequilibrated TIP3P water molecules (Jorgensen et al., 1983). Water molecules closer than 2.6 Å to atoms of the ReLPS were removed. Depending on the ReLPS conformation, 559–997 water molecules remained around the ReLPS molecule (cf. Table 1). The size of the water box was chosen to give a solvent layer of at least 6 Å around the ReLPS monomer. The resulting ensemble was energy minimized in two steps. First, the coordinates of the ReLPS were fixed and the water and the cations, if present, were energy minimized. In the second step, no constraints were applied and the whole ensemble was energy minimized.

TABLE 1 Number of hydrating water molecules and dimensions of ReLPS monomers

Conformation	Number of water molecules w/ Ca^{2+}	Number of water molecules w/o Ca^{2+}	Dimension (Å^3)
A	994	997	28 × 16 × 12
B	824	824	33 × 15 × 13
C	680	683	31 × 16 × 10
D	732	734	30 × 19 × 12
E	560	568	28 × 17 × 13
F	556	559	30 × 17 × 12

The integration time step was 1 fs. Bonds to hydrogen atoms were constrained using the SHAKE algorithm (van Gunsteren and Berendsen, 1977). Coordinates were saved at every 100th time step (0.1 ps), and neighborhood lists were updated every 10th time step. The cutoff radius was set to 12 Å. A shifted potential (Brooks et al., 1983) was used for the treatment of long-range interactions. Electrostatic interactions were evaluated using $\epsilon = 1$. Periodic boundary conditions were used in the x, y, and z directions (Allen and Tildesley, 1987). The ensemble was heated from 0 to 300 K in 10 ps and allowed to equilibrate for 10 ps. Only the final phase of 100-ps MD simulation was used for the evaluation of various properties.

In the following we describe the physical and geometrical parameters evaluated from the MD trajectories. The dynamic behavior of the ReLPS monomers was investigated in terms of glycosidic torsion angles, number of *gauche* defects n(GD) occurring in the acyl chains, extension (l) of these chains, order parameter (S_{CD}), and packing parameter (p).

The conformation of the headgroup was analyzed in terms of glycosidic torsion angles. Three successive bonds form the GlcN-I-GlcN-II and GlcN-II-KDO-I linkages. Two bonds connect KDO-I and KDO-II. The suite of atoms defining the torsions is indicated by asterisks in Fig. 2. The average torsion angles were computed from 1000 coordinate sets stored at 0.1-ps intervals and are given as the mean ± standard deviation (SD).

The average number of *gauche* defects of the acyl chains is related to the degree of order adopted by the hydrophobic part of the LPS. It was computed independently for subsequent 5-ps intervals to investigate its time dependency.

The extension l of the fatty acid chains reaches its maximum value in an all-*trans* conformation, which is found in the starting structures of the simulations. l is calculated from the distance between the first and the last carbon atom of the acyl chains.

The order parameter S_{CD} is a measure of the orientational order of the methylene groups of fatty acid chains, usually derived from NMR measurements (Seelig and Seelig, 1974). It is calculated from the angle θ between the C-H vector connecting carbon and hydrogen atoms of a methylene group and a vector normal to the membrane plane, using the following formula given by Seelig and Seelig (1974):

$$S_{CD} = \tfrac{1}{2}\,(3\langle\cos^2\theta\rangle - 1). \qquad (1)$$

Unfortunately, no membrane plane is defined when monomers are being investigated. Therefore, we defined a vector between the center of mass of the four sugar residues of the headgroup and the center of mass of the acyl chains. This vector substitutes the vector normal to the membrane plane usually used in these calculations and is used in the calculation of the headgroup area. Although this choice is arbitrary, the results can at least be compared among the different ReLPS conformers and ambient conditions investigated. Values of S_{CD} were averaged over intervals of 5 ps.

The packing parameter p describes the geometric properties of lipid molecules influencing the structure of supramolecular assemblies formed by these molecules (Israelachvili et al., 1980). Depending on the value of p, the formation of spherical micelles ($p < 1/3$), globular or cylindrical micelles ($1/3 < p < 1/2$), vesicles ($1/2 < p < 1$), planar bilayers ($p \approx 1$), or inverted micelles ($p > 1$) is predicted (Israelachvili et al., 1980). The packing parameter is calculated from

$$p = \frac{V}{a_0 l_c}, \qquad (2)$$

where V is the volume of the hydrophobic part (fatty acid chains), $V \approx (27.4 + 26.9n)$ Å^3; a_0 is the headgroup area, and l_c is the maximum or "critical chain length" of the fatty acid chains, $l_c = (1.5 + 1.265n)$ Å^3. We used the formulas given by Tanford (1972) for the estimation of V and l_c for saturated hydrocarbon chains with n atoms. Using parameters from

MEMBRANE (Kastowsky et al., 1991a), the headgroup area was calculated every 0.1 ps for each simulation from the projection of the headgroup along the vector between sugar residues and the acyl chains, which also substitutes the membrane normal in the calculation of the order parameter.

The properties of the water molecules solvating the ReLPS monomers were analyzed in terms of diffusion coefficients (D), radial distribution functions ($g(r)$), coordination numbers (n_{coor}), and mean residence times (τ).

The macroscopic diffusion coefficient D is related to the mobility of a molecule in solution. It can be calculated from the MD simulation using the following relations:

$$D = \frac{1}{3}\sum_{d=1}^{3}\frac{\Delta MSD_d}{2\Delta t} \tag{3}$$

with

$$MSD_d(t) = \langle |r_d(t) - r_d(0)|^2 \rangle, \tag{4}$$

where d is the spatial direction (x, y, z), $r_d(t)$ is the d-component of the coordinate vector at time t, and ΔMSD_d is the mean square displacement in the d direction. For comparison, the well-known Stokes-Einstein relation

$$D = \frac{kt}{6\pi\eta r} \tag{5}$$

(where k is Boltzmann's constant, T is the temperature in K, r is the radius of a spherical particle in m, and η is the viscosity ($\eta_{H_2O} = 0.89\ g\ m^{-1}\ s^{-1}$)) enables us to estimate the diffusion coefficient D, assuming a spherical shape of the ReLPS monomers. From the calculation of $D(H_2O)$, all water molecules were excluded that were located within the first hydration shell of the ReLPS monomer, because the diffusion of these molecules was assumed to be influenced by the solute (Hagler and Moult, 1978).

Radial pair distribution functions (RDFs) ($g(r)$) between water molecules and a hydrated ReLPS molecule give an impression of the structure and the size of the hydration shell. The ratio of the number $\Delta N(r)$ of solvent molecules found at a given distance from the solute to the number of solvent molecules that would be found in an ideal gas of the same density is calculated using

$$g_{ij}(r) = \frac{\Delta N(r)}{4\pi\rho_i r^2 \Delta r}, \tag{6}$$

where ρ_i is the density of the solvent, r is the radius, i denotes the solute, and j denotes the solvent, Δr is the interval for the calculation of g_{ij}, and $\Delta N(r)$ is the number of solvent molecules found in the distance interval $[r, r + \Delta r]$ from the solute.

RDFs were calculated between the oxygen atoms of the water molecules and hydrophobic and hydrophilic groups of the ReLPS monomers. The oxygen atoms of the carboxylate and phosphate groups were chosen as representatives of the hydrophilic groups, and the terminal methyl groups of the fatty acid chains represent the hydrophobic moiety. From comparison between RDFs of pure water and hydration water, the distortion of the bulk water properties induced by the amphiphilic solute can be deduced. Integration of $g(r)$ from $r = 0$ up to its first minimum gives the coordination number, i.e., the number of water molecules belonging to the first hydration shell of the solute.

Whereas RDFs and coordination numbers give an impression of the average static structure of the hydration shell, the mean residence time τ is a measure of the dynamics of the exchange of the hydration shell. To evaluate the influence of hydrophobic and hydrophilic regions of the ReLPS monomers on the mobility of solvent molecules, τ was calculated separately for these regions. Mean residence times were calculated according to the method described by Impey et al. (1983) and Garcia and Stiller (1993), using a probability function

$$n_i(t) = \frac{1}{N_t}\sum_{n=i}^{N_t}\sum_{j} P_{ij}(t_n, t, t^*), \tag{7}$$

where N_t is the number of time steps, t^* is the tolerance time, t is the time, and P_{ij} is a binary function, which equals 1 if the solvent molecule j is at time t and $t + t_n$ within the hydration shell of the solute molecule i, and did not leave the hydration shell for a time greater than t^* without meanwhile returning, otherwise P_{ij} equals 0. The tolerance time $t^* = 2$ ps minimizes the effect of rattling motions of solvent molecules leaving the solvent cage of the first hydration shell only for short times (Impey et al., 1983). The mean residence time τ is calculated from the decay of the function

$$n_i(t) = n_i(0)e^{-t\tau^{-1}}. \tag{8}$$

RESULTS

In the following, the results will be discussed in terms of averages of all ReLPS conformers investigated unless indicated.

Description of the conformations

The main features of the starting structures will be described here; for a more detailed description of these structures, the reader is referred to Kastowsky et al. (1993). The six acyl chains of the lipid A moiety are closely packed together in all-*trans* conformation. Three compact (A, B, C) and three elongated (D, E, F) acyl chain packing patterns were found (cf. Fig. 3). For all of the conformers investigated, a specific tilt angle of 53 ± 7° was found between the GlcN backbone and the fatty acid chains aligned in the z direction. Only two different orientations of the KDO dimer were energetically favored in vacuo, because they allowed the formation of a hydrogen bond to one of the phosphate groups of the lipid A moiety. The overall shape of the molecules is cylindrical, thus enabling a lamellar arrangement as found in the bacterial outer membrane (cf. also section under the heading Packing Parameter p, under Results).

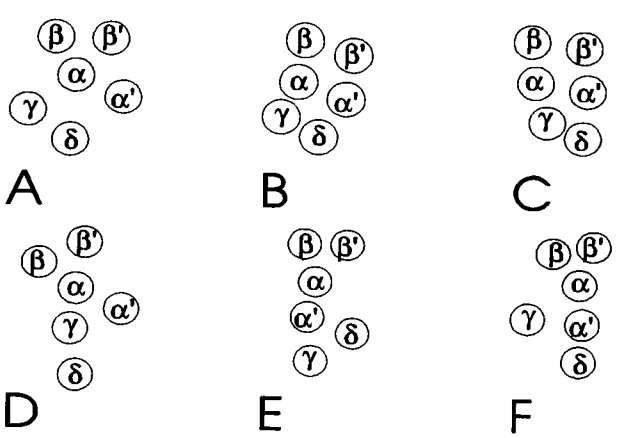

FIGURE 3 Packing patterns of the acyl chains of the starting structures of *E. coli* ReLPS. Greek characters denote the acyl chains as depicted in Fig. 2.

The favorite position of the calcium ions found by the grid search algorithm is between one of the negatively charged carboxylate groups of the KDO residues (KDO-I, KDO-II) and one of the phosphate groups connected to the GlcN backbone (GlcN-I, GlcN-II). An example of the resulting structure is given in greater detail in Fig. 4. In Table 2 the position of the calcium cations with respect to the negatively charged groups of the ReLPS is given.

The overall structure of the ReLPS conformers is conserved during the simulations. The hydrophobic region retains a compact structure. The group of four acyl chains (α, α', β, β') attached to GlcN-II is conformationally more stable than the group of two acyl chains (δ, γ) linked to GlcN-I. For all ReLPS conformers investigated, the flexibility of the headgroup is decreased in the presence of the Ca^{2+} ions.

In Fig. 5, selected snapshots taken at 0, 50, and 100 ps after the end of the equilibration phase from two simulations (C-Ca, D-Ca) conducted in the presence of Ca^{2+} ions are depicted. The order of the acyl chains of C-Ca does not decrease significantly during the simulation. The chains are arranged in parallel. Only the terminal methyl and methylene groups show some flexibility. In the headgroup region, only minor changes can be noted. A carboxylate-calcium-phosphate bridge can be found between KDO-I and GlcN-II. No such bridge can be found for KDO-II, which consequently shows larger fluctuations. On the other hand, D-Ca shows significant distortion of the ordered structure of the acyl chains after 50 ps, which still increases toward the end of the simulation phase. Two chains (δ, γ) connected to GlcN-I are strongly bent and cross the remaining four chains (α, α', β, β') connected to GlcN-II at an angle of almost 90° after 100 ps. The headgroup region of D-Ca is rigidified by the presence of two carboxylate-calcium-phosphate bridges between KDO-I and GlcN-II and KDO-II and GlcN-I.

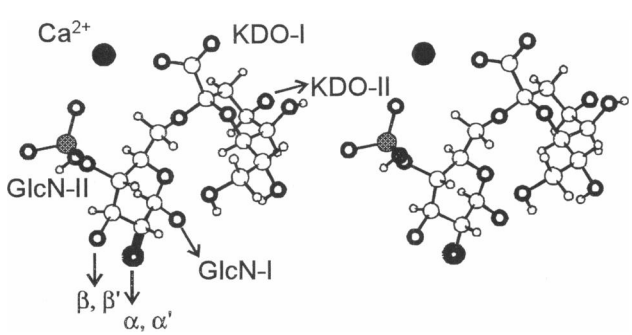

FIGURE 4 Detail of the headgroup of E taken after 15 ps. The calcium cation (*black*) is located between the 4′-phosphate group at GlcN-II and the carboxylic group at KDO-I. The rest of the ReLPS molecule is omitted for clarity, linkages to KDO-II, GlcN-I, and the acyl chains at GlcN-II are indicated by arrows. Calcium: black; carbon: circles with thin lines; oxygen: circles with thick lines; hydrogen: small circles; phosphate: gray; nitrogen: black circle with white dot. Arrows indicate bonds to KDO-II, GlcN-I, and acyl chains (α, α', β, β'). The stereo plot was generated with SCHAKAL (E. Keller, Freiburg, Germany).

TABLE 2 Position of the calcium cations found by the grid search

Conformation	1. Ca^{2+}	2. Ca^{2+}
A-Ca	GlcN-I/KDO-II	KDO-I
B-Ca	GlcN-I/KDO-I	GlcN-II/KDO-II
C-Ca	GlcN-I	GlcN-II/KDO-I
D-Ca	GlcN-I/KDO-I	GlcN-II/KDO-II
E-Ca	GlcN-I/KDO-II	GlcN-II/KDO-I
F-Ca	GlcN-I	GlcN-II/KDO-I

The numbering of the cations (1, 2) is arbitrary. GlcN-KDO refers to a phosphate-calcium-carboxylate bridge, whereas GlcN or KDO alone indicates the absence of such a bridged structure.

These observations are in contrast to the behavior of the same conformations (C, D) in the absence of Ca^{2+} ions, as can be seen in Fig. 6. The order of the fatty acid chains of C slightly decreases during the simulation, and the headgroup region was more compact at the end of the simulation. The motions of the headgroup are significantly increased as compared to C-Ca. D achieved a high state of order of the acyl chains after 100 ps, but the relative orientation between the backbone region and the direction of acyl chains was

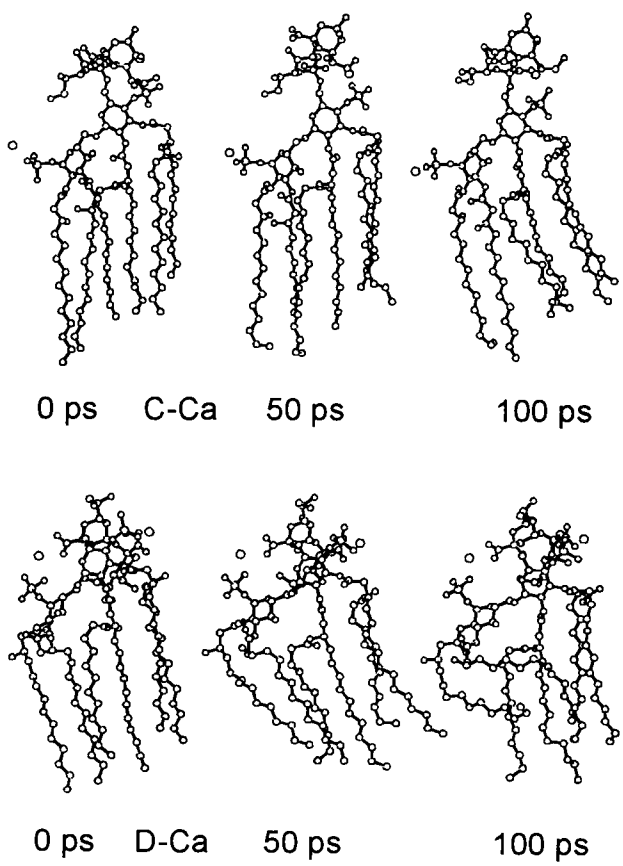

FIGURE 5 Snapshots taken from the simulations C-Ca (*top*) and D-Ca (*bottom*) of ReLPS carried out in the presence of Ca^{2+} ions. As indicated below the structures, the pictures were taken at 0 ps, 50 ps, and 100 ps after the end of the equilibration phase. Hydrogen atoms are omitted for sake of clarity.

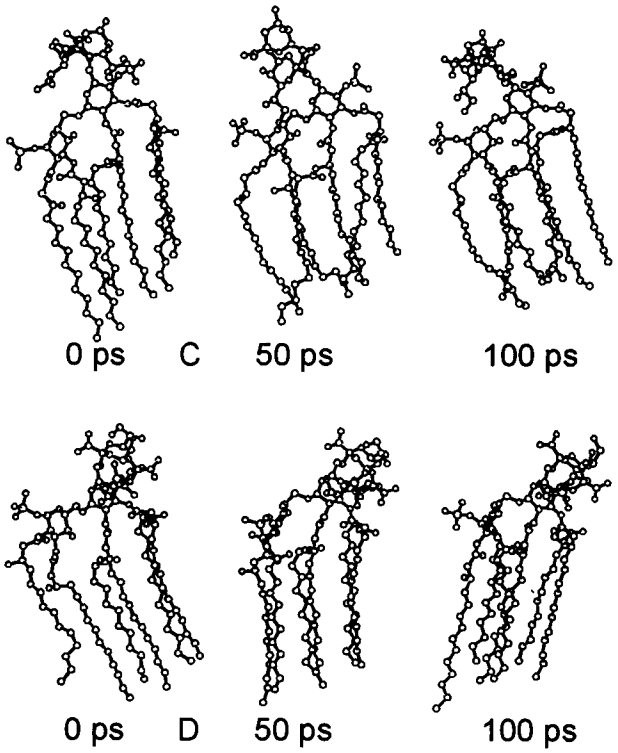

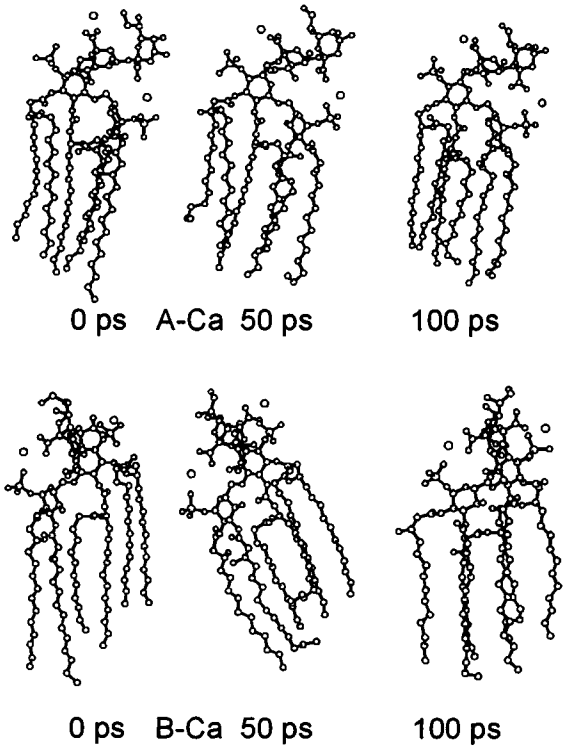

FIGURE 6 Snapshots of the same ReLPS conformations C (*top*) and D (*bottom*) as in Fig. 5, simulated in the absence of Ca^{2+} ions.

changed. The changes in the headgroup conformation are more obvious for D than for D-Ca.

The effect of the Ca^{2+} ions on the conformational flexibility was less pronounced for conformations A and B, as can be seen in Fig. 7. The acyl chains were more flexible and thus showed more kinks in the absence of calcium ions than in their presence. A carboxylate-calcium-phosphate bridge between KDO-II and GlcN-I stabilizes the headgroup conformation of A-Ca, whereas two bridges can be found for B-Ca (cf. Table 2).

Glycosidic torsions

In Table 3, mean torsion angles for the glycosidic linkages GlcN-I-GlcN-II, GlcN-II-KDO-I, and KDO-I-KDO-II are listed. Interestingly, for most of the torsions only a few different angles were found (cf. Fig. 8). The largest variety of torsion angles was found for the first two torsions of the GlcN-II-KDO-I linkage, whereas its third torsion remained constant. Unexpectedly, the motion of the outermost groups, involving the KDO-I–KDO-II linkage, is rather limited.

The small standard deviation from the mean indicates a limited flexibility of the torsions. As indicated in Table 3, for three simulations (C, D, and F) the angle distribution of one torsion showed two peaks, resulting from a transition between two favored angles during the simulations. In these cases, average torsion values are misleading.

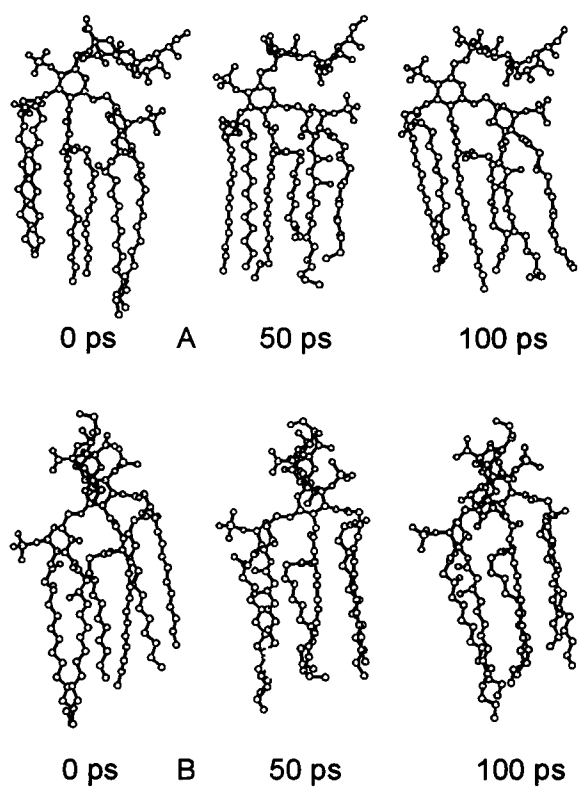

FIGURE 7 Snapshots of ReLPS conformations A and B, simulated in the presence (*top*: A-Ca, B-Ca) and absence (*bottom*: A, B) of Ca^{2+} ions.

TABLE 3 Mean glycosidic torsion angles in the absence and presence of Ca^{2+} ions

			A		B		C		D		E		F	
			Angle	SD	Angle	SD	Angle	SD	Angle	SD	Angle	SD	Angle	SD
GlcN-I	-GlcN-II	(OCCO)	−74	13	−68	12	−62	12	−62	17	−47	11	−56	11
GlcN-I	-GlcN-II	(CCOC)	−158	9	−168	9	−171	12	**−142	30	−158	12	***−149	23
GlcN-I	-GlcN-II	(COCO)	−70	12	−74	12	−75	11	−69	17	−53	13	−59	13
GlcN-II	-KDO-I	(OCCO)	47	11	−46	11	*81	19	−51	9	69	12	47	10
GlcN-II	-KDO-I	(CCOC)	−174	11	161	10	−153	7	−173	8	−170	9	106	14
GlcN-II	-KDO-I	(COCO)	52	8	48	8	64	10	55	8	59	9	52	10
KDO-I	-KDO-II	(CCOC)	−117	13	−147	9	−156	11	−138	9	−148	10	−154	14
KDO-I	-KDO-II	(COCO)	177	8	49	8	42	8	53	7	46	8	45	11
			A-Ca		B-Ca		C-Ca		D-Ca		E-Ca		F-Ca	
			Angle	SD	Angle	SD	Angle	SD	Angle	SD	Angle	SD	Angle	SD
GlcN-I	-GlcN-II	(OCCO)	−61	10	−49	12	−76	16	173	10	−45	11	−62	9
GlcN-I	-GlcN-II	(CCOC)	−160	11	167	12	−161	12	−160	10	−168	10	−131	16
GlcN-I	-GlcN-II	(COCO)	−66	11	−66	13	−75	13	50	10	−52	11	−63	10
GlcN-II	-KDO-I	(OCCO)	50	11	−68	12	153	12	−59	7	52	8	87	7
GlcN-II	-KDO-I	(CCOC)	−166	13	162	9	−173	15	162	9	−164	7	130	8
GlcN-II	-KDO-I	(COCO)	57	8	41	10	54	8	45	9	53	7	52	8
KDO-I	-KDO-II	(CCOC)	−85	13	−120	9	−154	13	−116	10	−153	8	−146	14
KDO-I	-KDO-II	(COCO)	65	8	61	7	47	9	66	8	50	7	51	11

Stars indicate two peaks of the angular distribution function: *, 75/125; **, −175/−105; ***, −165/−135.
For each simulation the mean torsion angle (°) and its standard deviation (SD) were obtained from averaging 1000 coordinate sets representing 100-ps simulation time. The four atoms defining a torsion are given in parentheses after the name of the glycosidic linkage (GlcN-I-GlcN-II, GlcN-II-KDO-I, KDO-I-KDO-II), referring to the atoms marked by asterisks in Fig. 3.

Number of *gauche* defects *n*(GD)

Because of the highly ordered starting structures with completely extended acyl chains aligned parallel to each other, the percentage of *gauche* defects was 0 at the beginning of the MD simulations and increased during the course of the simulation. After 100 ps, an average value for all acyl chains of all ReLPS monomers of 2–2.5% was reached (cf. Fig. 9). Although the number of *gauche* defects was lower in the absence of calcium cations in the beginning, the difference vanished at the end of the simulation phase. After approximately 85 ps, no further increase in the overall average of n(GD) was observed. The maximum value of 5.9% was observed after 90 ps during the simulation of D-Ca, whereas in the absence of cations C reached a maximum value of 4.5%. A closer investigation of the evolution of n(GD) of the different chains of one ReLPS conformer revealed strong differences between the chains. During the simulation of E (cf. Fig. 10), the maximum value of n(GD) = 14% was observed after 90 ps for the δ-acyl chain. On the other hand, no *gauche* torsion was detected in the α-chain during the first 65 ps of the simulation. For this acyl chain, n(GD) never exceeded 3.5% during the entire simulation. After 15 ps, n(GD) of the α'-acyl chain reached a first maximum of 4%, then decreased to 0% and went up to 4% again after 80 ps. It took 60 ps before the average value of n(GD) of all chains of E exceeded 1%.

Extension *l* of the acyl chains

As can be seen in Fig. 11, the apparent length l of the acyl chains decreased during the course of the simulation for all conformers, except D, where it reached its starting value again after some intermediate fluctuations. In the presence of Ca^{2+}, l decreased for D-Ca by ~1.5 Å. On the other hand, the decrease in l was stronger for F than for F-Ca. In the case of A and C, the evolution of l in time was similar in the presence and absence of calcium cations. Although the shortening of the apparent acyl chain length occurred 40 ps later for E than for E-Ca, after 100 ps the same chain length was found. The strong initial decrease in l occurring during the simulation of B-Ca was fully compensated after 70 ps.

Order parameter of the acyl chains

The acyl chain order parameter $S = |S_{CD}|$ is depicted in Fig. 12 as a mean value for all acyl chains of each ReLPS conformer in the presence and absence of calcium cations. Starting from a value of 0.2–0.3 at the first methylene group, S increases to about 0.4 in the middle of the acyl chains and decreases again toward the end of the chains to values below 0.2. The SD calculated from the averaging procedure carried out for all acyl chains was highest at the beginning and the end of the acyl chains and lowest in the middle. Maximum values of S corresponded to minimum values of SD. Only minor differences in S were found in the presence and absence of calcium cations for A/A-Ca and F/F-Ca, respectively. In both cases, the order parameter profiles in the presence and absence of calcium intersect at an intermediate carbon number. S(C) was lower than S(C-Ca), whereas for B, D, and E, S was higher in the absence of Ca^{2+} than in its presence.

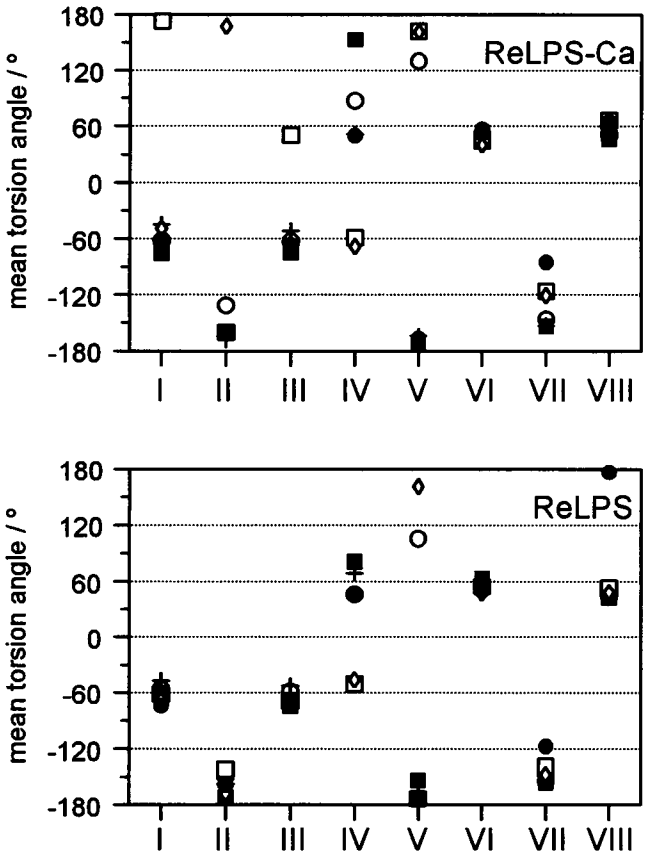

FIGURE 8 Mean glycosidic torsion angles of the linkages GlcN-I-GlcN-II, GlcN-II-KDO-I, and KDO-I-KDO-II in the presence (*top*) and absence (*bottom*) of calcium ions. Torsion angles are given in degrees. The four atoms defining a torsion are given in parentheses, referring to the atoms marked by asterisks in Fig. 2. I: GlcN-I-GlcN-II (OCCO); II: GlcN-I-GlcN-II (CCOC); III: GlcN-I-GlcN-II (COCO); IV: GlcN-II-KDO-I (OCCO); V: GlcN-II-KDO-I (CCOC); VI: GlcN-II-KDO-I (COCO); VII: KDO-I-KDO-II (CCOC); VIII: KDO-I-KDO-II (COCO). A, A-Ca: filled circles; B, B-Ca: diamonds; C, C-Ca: filled squares, D, D-Ca: open squares; E, E-Ca: crosses; F, F-Ca: open circles.

Packing parameter *p*

In Table 4, mean values of the packing parameter p are listed for the six different conformations. p was constant during the simulation, reaching values between 0.8 and 1.1, with the exception of A/A-Ca, where temporarily a maximum of 1.3 was observed. The average headgroup area was 146 ± 12 Å^2 in the presence and 150 ± 13 Å^2 in the absence of Ca^{2+}.

Diffusion coefficient *D*

The average value of D(ReLPS) was calculated to be on the order of 0.1×10^{-9} m^2/s. Taking into account the large standard deviation obtained from the averaging of the values of D(ReLPS) calculated for different time intervals, no difference was detected between the different conformers. Moreover, no effect of the presence of calcium ions could be seen.

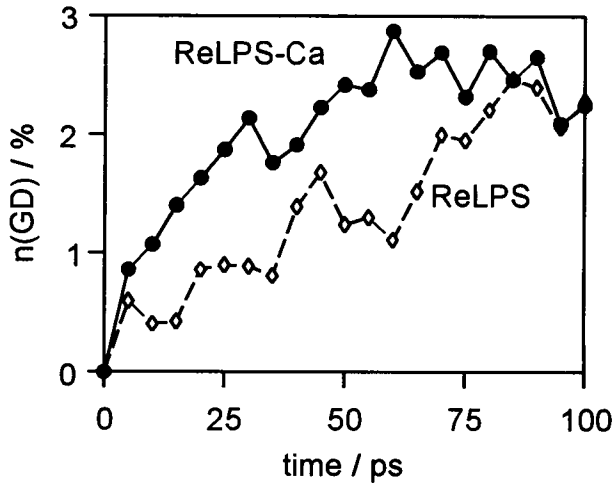

FIGURE 9 The average number n(GD) of *gauche* defects of all fatty acid chains of all ReLPS conformers investigated in the presence (*solid line*) and absence (*dashed line*) of calcium cations.

For the surrounding water molecules, an average value of $D(H_2O) = (2.6 \pm 0.2) \times 10^{-9}$ m^2/s was observed both in the presence and absence of calcium ions. This can be explained by the exclusion of water molecules closer than 4 Å to any atom of the ReLPS (or ReLPS/Ca^{2+} complex, respectively) from these calculations. The radius of the average first hydration shell of the ReLPS molecules is based on the position of the first minimum of the RDF of different atomic groups in the ReLPS molecules (cf. next paragraph). The diffusion coefficient calculated for the calcium ions $D(Ca^{2+}) = (0.2 \pm 0.2) \times 10^{-9}$ m^2/s was slightly higher than D(ReLPS).

Radial pair distribution functions

In Fig. 13, RDFs between water molecules and selected atoms of the ReLPS molecules are depicted. The RDF was more pronounced for the negatively charged oxygen atoms of the headgroup than for the neutral carbon and hydrogen atoms of the hydrophobic region. Up to four maxima could be detected in the oxygen-oxygen RDF, whereas not more than two maxima could be distinguished for the nonpolar

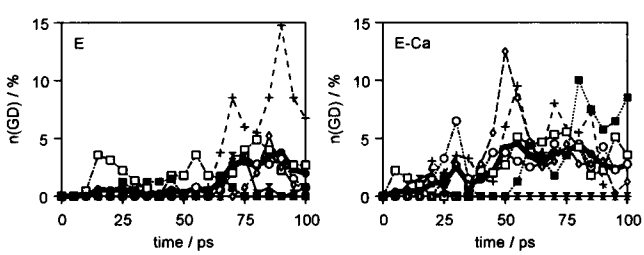

FIGURE 10 The average number n(GD) of *gauche* defects occurring in the acyl chains of ReLPS-conformation E in the absence (*left*) and presence (*right*) of calcium cations. Numbering of the chains according to Fig. 2: α: hourglass; α': diamond; β: filled square; β': open square; δ: cross; γ: open circle; mean value of chains 1–6: thick line with closed dots.

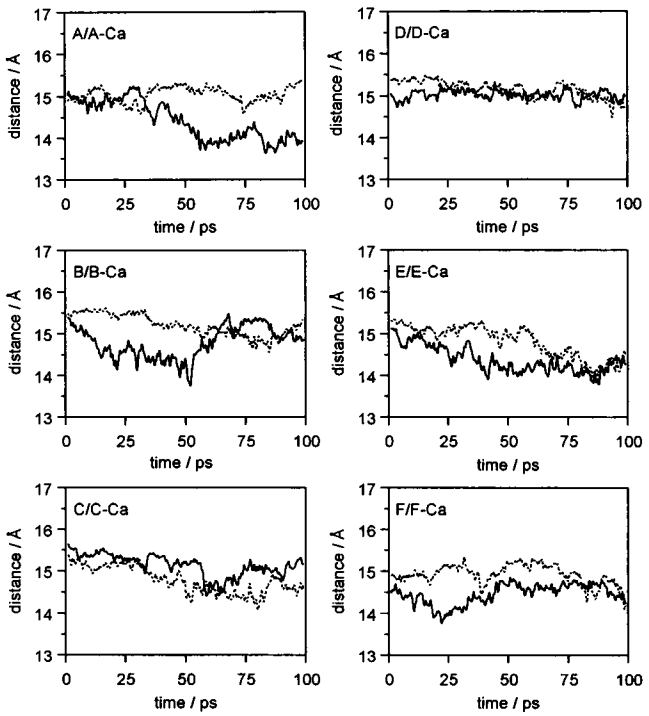

FIGURE 11 The average distance between the first and the last atom of all acyl chains of the ReLPS conformers A-F versus time in the presence (*solid lines*) and absence (*dashed lines*) of Ca^{2+} ions. The time is given in picoseconds, the distance is in angstroms.

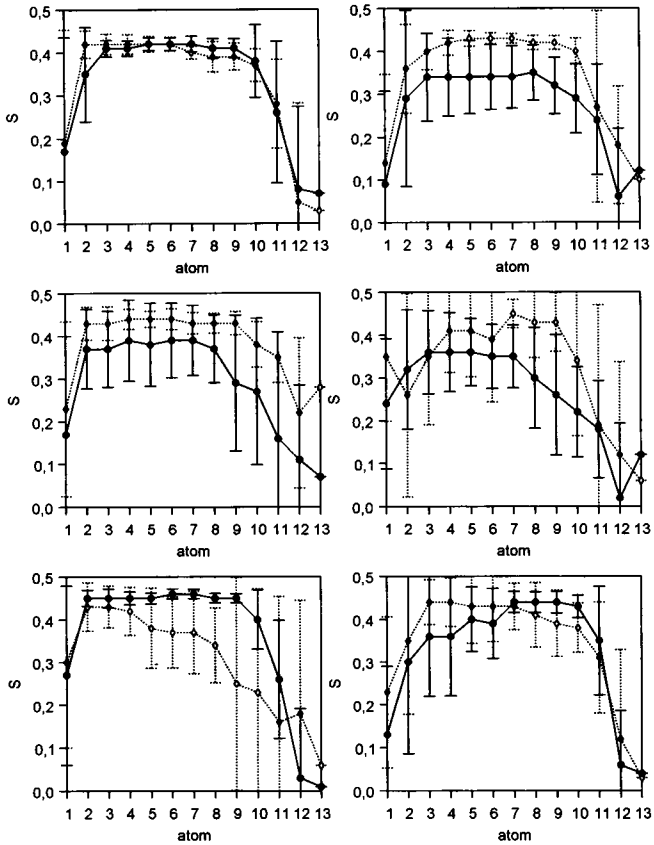

FIGURE 12 Profiles of the average order parameter $S = |S_{CD}|$ of all acyl chains of ReLPS conformers A-F computed from simulations with (*solid lines*) and without (*dashed lines*) cations present. Error bars denote the standard deviation of the calculated mean values. (Top: *A, D*; middle:*B, E*; bottom: *C, F*).

atoms. The first maximum was reached at $r = 2.8–3.1$ Å for the oxygen atoms and $r = 2.9–3.4$ Å for the hydrogen atoms. It was shifted to larger distances ($r = 3.6–3.8$ Å) for the terminal carbon atoms of the acyl chains. The peaks were highest for carboxylic oxygen atoms and phosphate oxygen atoms, reaching values of ~1.8. The peak was smallest for the hydrogen RDF, where a value of 0.6–0.8 was reached. For the terminal carbon atoms, the peak height did not exceed 0.8.

Coordination numbers

For the oxygen atoms of the charged groups of the ReLPS monomers, an average coordination number of 5 water molecules per atom was determined from the RDF. For the carbon atoms of the terminal methyl group, coordination numbers ranging from 7.8 to 8.7 were obtained.

Mean residence times τ

In Table 5, mean residence times τ of water molecules in the vicinity of different regions of the ReLPS molecules are listed. The presence of calcium leads to an increase in residence times τ of water molecules in the hydrophilic region of the ReLPS molecules by ~50% but does not influence τ in the hydrophobic part. This observation was even more drastically supported by an investigation of residence times close to the different atomic groups defined in the previous section. Whereas for the terminal carbon atoms of the acyl chains, $\tau = 9.3$ ps and $\tau = 8.9$ ps was measured without and with Ca^{2+} ions present, respectively, for the carboxylic oxygen atoms values of $\tau = 10.1$ ps and 69.2 ps were observed. For the oxygen atoms of the phosphate groups, the difference was even more drastic: τ increased from 12.6 ps to 130.9 ps upon the presence of calcium cations. For these calculations, different radii of the first hydration shell were assumed for the different atoms (cf. Table 5), based on the evaluation of the RDFs. When Ca^{2+} ions were present, some of the water molecules did not leave the hydration shell of the charged oxygen atoms during the entire simulation time of 100 ps, whereas the

TABLE 4 Mean packing parameter (± standard deviation) of ReLPS monomers

w/o Ca^{2+}	$V/(a_0 \times l_c)$	w/ Ca^{2+}	$V/(a_0 \times l_c)$
A	0.92 ± 0.09	A-Ca	1.02 ± 0.11
B	0.85 ± 0.04	B-Ca	0.90 ± 0.05
C	0.84 ± 0.03	C-Ca	0.85 ± 0.03
D	0.73 ± 0.02	D-Ca	0.81 ± 0.02
E	0.83 ± 0.02	E-Ca	0.82 ± 0.02
F	0.91 ± 0.05	F-Ca	0.83 ± 0.02

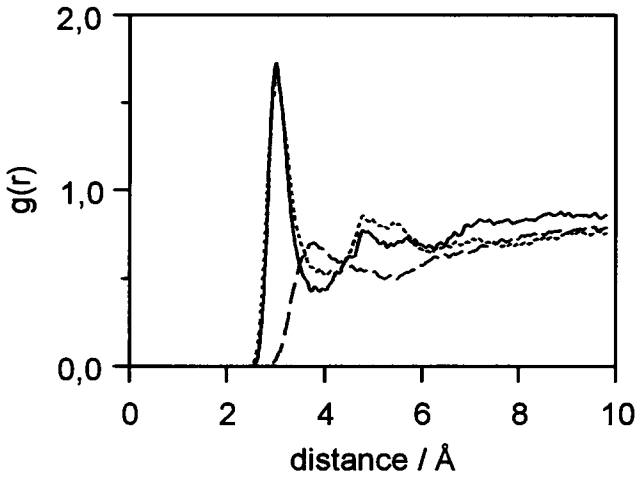

FIGURE 13 Radial distribution functions of water molecules in the vicinity of different atomic groups of the ReLPS F-Ca in the presence of Ca^{2+} ions. The distance is given in angstroms. Solid line: $O_{carboxylate}$; dotted line: $O_{phosphate}$; dashed line: C_{methyl}.

TABLE 5 Mean residence times τ of water molecules in the hydration shell of ReLPS molecules

ReLPS region	Hydration shell radius (Å)	τ w/ Ca^{2+} (ps)	τ w/o Ca^{2+} (ps)
$O_{carboxylate}$	4.0	69.2	10.1
$O_{phosphate}$	4.0	130.9	12.6
C_{methyl}	5.0	8.9	9.3
Hydrophilic	4.0	29.8	22.6
Hydrophobic	4.0	15.9	16.1

$O_{carboxylate}$, Average of four oxygen-water RDFs.
$O_{phosphate}$, Average of two phosphate-water-RDFs.
C_{methyl}, Average of six carbon-water-RDFs (terminal methyl groups of the acyl chains).
Hydrophilic region, Charged headgroup (GlcN-I, GlcN-II, KDO-I, KDO-II).
Hydrophobic region, Acyl chains.

maximum residence time observed without calcium present was 81.3 ps.

DISCUSSION

The preferred position found for the Ca^{2+} ions is between the negatively charged carboxylic and phosphate groups (cf. Fig. 4), resulting in a stable bidentate complex. Holst et al. (1993) proposed a similar salt-stabilized structure for a core fragment of *Chlamydia* LPS subjected to mass spectrometric analysis. This calcium position also complies with calculations by Sabisch (1994), who compared electron density profiles derived from molecular models including water and cations to those obtained by x-ray diffraction of multilamellar aggregates of ReLPS. The cation fixes the distances between the negatively charged groups and thus stabilizes and rigidifies the intramolecular structure of both the backbone and the core region. Intermolecular rigidification of phospholipid aggregates by virtue of cation-phosphate-water bridges was reported by Hauser (1973). Coughlin et al. (1985) found a significant effect of ionic bridges within lipopolysaccharide aggregates on the headgroup motion and the LPS aggregation state.

The presence of calcium altered the conformation of the GlcN residues, thus changing the packing and the intramolecular distances of the acyl chains. Because of the limited flexibility of the amide and ester linkages connecting the backbone to the acyl chains, small motions of the GlcN backbone in some simulations resulted in significant distortions of the acyl chain packing and acyl chain order.

The overall structure of the ReLPS molecules was preserved during the simulations, although both the headgroup and the hydrophobic region showed some flexibility. The ReLPS molecules were not trapped in a local energy minimum, but were enabled to adopt different conformations. Nevertheless, no transition between the different structures was observed. To observe such a transition, presumably more simulation time or a different simulation setup (simulated annealing) is necessary.

The flexibility of the headgroup torsions was rather limited, as expressed by small standard deviations of mean glycosidic torsion angles. Transitions between different values were observed in only three simulations out of 12. The observed changes in the overall structure of the headgroup during the simulations thus presumably required a concerted modification of a number of torsions at the same time.

Surprisingly, at the glucosamine backbone, a transition between two different angles was observed during the simulations D and F, although the motion of the backbone sugar residues was expected to be limited by the attached fatty acids on the one hand and the KDO core on the other. These transitions occurred exclusively in the absence of calcium, stressing the rigidifying effect of Ca^{2+} ions on the ReLPS conformations.

A typical set of torsion angles, going from GlcN-I to KDO-II, was −60, −160, −65, (*), −168, 52, 50, −140°. As indicated by (*), no typical value can be given for the O-C-C-O torsion at the GlcN-II-KDO-I linkage, because a number of different angles were observed here. Conformations C and E fit best to this set of typical torsions.

No direct comparison can be made to simulations and experimental results derived from experiments on aggregated lipids, usually forming bilayers or micelles, because no biophysical investigations have been carried out yet for the monomeric state, chosen here for the investigation of ReLPS. Usually the phospholipids experience an environment, especially in the hydrophobic region, where no water is found (e.g. Chiu et al., 1995), which is different from the environment of isolated ReLPS molecules studied in the present work.

The extension of the acyl chains was reduced during the simulations because of the introduction of *gauche* bonds into the chains, which were in all-*trans* conformation before. This occurred both close to the linkage to the backbone and, especially, at the end of the chain. For aggregated phospholipids it has long been known that the terminal

methylene groups show the largest flexibility (Hauser, 1973).

The small number of *gauche* defects (n(GD) = 2.5%) found in the acyl chains of the ReLPS is indicative of a highly ordered structure, which is adopted by aggregated phospholipids in the gel phase. For 1,2-dipalmitoyl-*sn*-glycero-3-phosphocholine (DPPC) membranes below the phase transition temperature, n(GD) = 10.9, 1.7, and 2.5% was found for 4-, 6-, and 10-d_4-DPPC, respectively, whereas above the phase transition temperature, values of n(GD) = 20.7, 32.3, and 19.7% were observed at these positions (Mendelsohn et al., 1989). Our simulation temperature of T = 300 K is at the lower limit of the gel-to-liquid crystalline phase transition temperature of ReLPS, as observed by Seydel et al. (1993) and Brandenburg et al. (1993). Therefore, the acyl chain structure of the ReLPS during the simulation may be best described as gel phase-like.

The order parameter S of the acyl chains measures the alignment of the acyl chains parallel to a membrane normal. In Fig. 14, averaged order parameter profiles from our simulations are compared to the theoretical profile reported by Israelachvili et al. (1980) for aggregated phospholipids. In the literature, order parameters were reported to depend on the temperature (Seddon et al., 1983), on the aggregation phase of the membrane (Gally et al., 1979), and on the global tilt of the acyl chains (Gally et al., 1980). The chosen simulation temperature of 300 K is below the phase transition temperature of aggregated ReLPS, whereas the phase state of monomeric ReLPS has not been investigated yet. Again, we have to stress that the monomeric ReLPS cannot readily be compared to aggregates of phospholipids. Because of the lack of a membrane normal at the ReLPS monomers, an internal reference vector was computed. Therefore, a general tilt of the acyl chains versus the headgroups could not detected by our procedure. For lamellar aggregates of LPS a tilt of ~10° was estimated (Sabisch, 1994), which was not included in the calculations of S_{CD}.

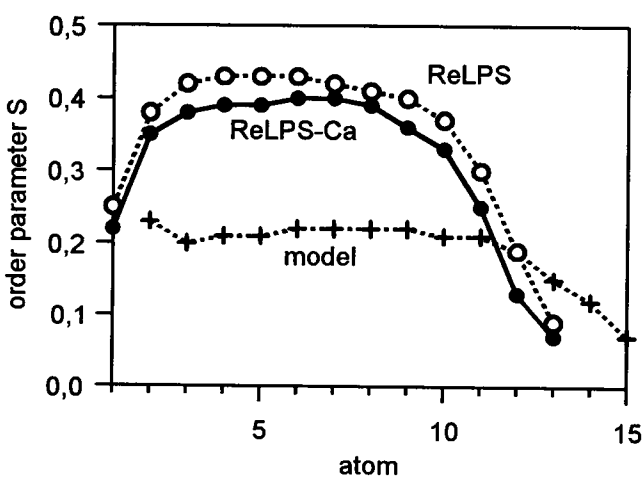

FIGURE 14 Comparison between order parameters $S = |S_{CD}|$ determined for ReLPS and model calculations for aggregated phospholipids (Israelachvili et al., 1980). For ReLPS, an average of all conformers is given both in the presence (*closed circles*) and absence (*open circles*) of calcium cations.

In general, for bilayers of simple phospholipids it was found that the order parameter remains relatively constant along the chain and decreases only near the end of the chain (Israelachvili et al., 1980). For ReLPS, the order parameter starts from low order at the beginning of the acyl chains, increases in the middle, and decreases again near the end of the chains. This discrepancy between the profiles of the order parameter of LPS and of aggregated phospholipids is probably due to the more complex structure of LPS as compared to phospholipids like DPPC. Usually, low order parameters are explained as resulting from the averaging of many different conformations of a methylene group, but they can also result from a fixed angle. For example, S_{CD} = 0 is measured for an isotropically tumbling segment in a NMR experiment, as well as for a segment fixed at an angle of 54.7°. The conformation of the first methylene groups is dominated by their linkage to the GlcN backbone, and thus their flexibility is decreased. They are forced into a position that results in a low order parameter, although they are not free to move.

As confirmed by visual inspection, the methylene groups in the middle of the chains adopt a highly linear and ordered structure, presumably due to the presence of neighboring acyl chains. The flexibility increases toward the end of the chains, where kinks and *gauche* defects result in a decreased order of the acyl chains and thus in a decreased order parameter.

Gally et al. (1980) noted an increase in the order parameter of multilamellar aggregates of phospholipids in the presence of bivalent cations. This is in contrast to our observation that on the average of all monomeric ReLPS conformers investigated, the presence of calcium ions resulted in a slightly reduced order of the hydrophobic domain, although the differences were within the range of the standard deviation. This discrepancy might again indicate that ReLPS in the monomeric state, where cations form intramolecular bridges, cannot readily be compared to aggregates of phospholipids, which are bridged intermolecularly by cations.

We observed a high state of order of the hydrophobic domain of the ReLPS monomers, as found earlier for ReLPS aggregates by Labischinski et al. (1985). This might be explained by the specific structure of LPS. Simple phospholipids consist of two acyl chains, whereas each ReLPS monomer carries six fatty acid chains, which can adopt a compact, micro-membrane-like structure. This term reflects the strong tendency of the acyl chains to adopt a highly ordered, membrane-like structure in parallel alignment. Moreover, the highly ordered fatty acid region of the ReLPS molecules might explain the observation of Nichol et al. (1980), that phospholipids of the outer membrane, in which LPS are present, adopt higher ordered structures than the phospholipids of the cytoplasmic membrane, which is devoid of LPS.

An average headgroup area of $a_0 = 148 \pm 12$ Å^2 was calculated, whereas by monolayer studies of highly purified *E. coli* ReLPS, $a_0 = 140 \pm 9$ Å^2 was determined (Kahle and Koch, unpublished results). The small discrepancy is well tolerated, taking into account that the calculated headgroup area is obtained from the projection of the headgroup on the membrane plane, i.e., it defines the maximum area required by the headgroup, neglecting interdigitation of elements of neighboring headgroups. The headgroup area was slightly smaller in the presence of calcium ions, but the difference is within the range of the standard deviation.

The supramolecular structure of various preparations of LPS has been the studied intensely in the past (see Seydel et al., 1993, and references therein), and there has been evidence of both lamellar (e.g., Labischinski et al., 1990) and nonlamellar (e.g., Brandenburg, 1993) LPS aggregates. It has been suggested that the endotoxic potency of a given lipid A sample was directly related to its ability to adopt nonlamellar structures (Brandenburg et al., 1993). Our results for the packing parameter p of the ReLPS monomers, which were shown to be potent stimulators of the immune response in vitro (Takayama et al., 1994), are well within the range 0.5–1, which is thought to be indicative of lamellar structures (Israelachvili et al., 1980). With the exception of simulations A and A-Ca, no values of p indicating a tendency to adopt nonlamellar structures were found. During the simulations A and A-Ca, values of $p > 1.0$, pointing to a preference for inverted micellar structures, were found only for ~10% of the simulation time. Therefore, the ReLPS monomers are most likely to form lamellar aggregates under the conditions investigated in this study. This is consistent with the observation reported by Seydel et al. (1993), that in the presence of divalent cations, nonlamellar structures were suppressed below the phase transition temperature T_c, which is higher than the simulation temperature of $T = 300$ K.

The different structures of the RDFs of different atomic groups in the ReLPS molecules point to differences of the structure of the hydration shells of hydrophobic and hydrophilic regions. In contrast to RDFs of monoatomic ions, where $g(r)$ oscillates around 1 for large distances ($r > r$(first hydration shell); Obst and Bradaczek, 1996), we observed $g(r) < 1$ for the ReLPS atoms. This is due to the nature of the formula used in this kind of calculation, which is essentially based on the assumption of a spherically hydrated atom freely accessible for water molecules from all directions. This is true for single Ca^{2+} ions, for example, but not for atoms that are part of a (macro) molecule. The part surrounding the atom where no water molecules can be found because it is occupied by atoms of the macromolecule, would have to be excluded from the normalization of the $g(r)$ function. A suitable procedure taking into account the accessible volume has been developed recently by Leroux et al. (1995). The presence of Ca^{2+} ions leads to an altered structure of the RDF, as can be seen from Fig. 15. The second maximum of the RDF is far more pronounced in the presence of the cations close to the carboxylate oxygen

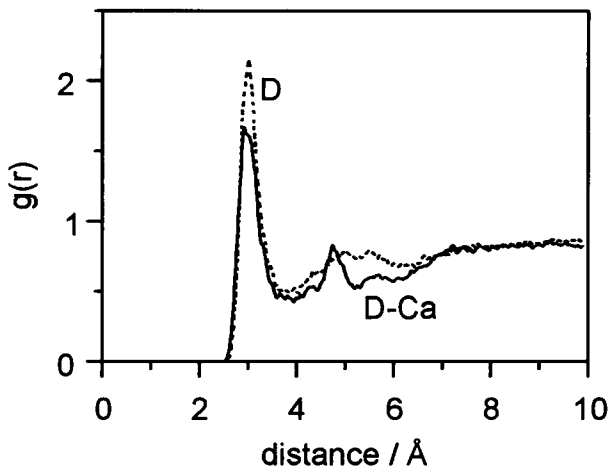

FIGURE 15 Radial distribution functions of water molecules in the vicinity of the carboxylate groups of an ReLPS conformer in the presence (D-Ca, *solid line*) and absence (D, *dotted line*) of calcium cations. The distance is given in angstroms.

atoms, whereas the first maximum is slightly reduced. This could be interpreted in terms of a stronger hydration of the carboxylate groups due to the presence of calcium, although no change of the coordination number of the first shell was detected. This view is supported by the increase in mean residence times noted when Ca^{2+} was present.

In the hydrophobic region of the ReLPS molecules, the structure of the RDF was less pronounced than in the hydrophilic headgroup region. This can be explained by the lack of attractive forces between the weakly polarized hydrocarbon chains and the water molecules, whereas the negative charges located at the carboxylate and phosphate groups and the positive charges of the Ca^{2+} ion exert a strong influence on the structure of the water, which extends farther into the solvent.

The mean residence time of water molecules solvating the ReLPS molecules can be compared to the results obtained for proteins by experimental and theoretical methods (Brooks and Karplus, 1989; Otting et al., 1991; Brunne et al., 1993), because proteins, unless they are incorporated in a membrane, usually are completely solvated.

In the vicinity of the bovine pancreatic trypsin inhibitor (BPTI), Otting experimentally found mean residence times in the range of 100–300 ps. These results are comparable to those obtained for the hydration of the carboxylic and phosphate groups of ReLPS, but are higher than the mean residence times of the hydrophobic region of ReLPS. For the same protein, BPTI, Brunne found by MD simulation that the residence times were higher in the vicinity of polar amino acids compared to nonpolar or charged side chains.

As compared to bulk water, the mean residence times are increased approximately fivefold in both the hydrophilic and the hydrophobic regions of the ReLPS molecules. One reason might be a sterical hindrance introduced by the mere presence of the ReLPS molecule, which limits the volume accessible for diffusing water molecules, as discussed for phospholipids by Hauser (1973).

The residence times were higher in the headgroup region, where the partial charges carried by the water molecules could interact with the (partial) charges of the headgroup atoms. For phospholipid aggregates, Hauser (1973) found that the phosphate groups governed the solvation shell dynamics, which is in accord to our observation that the residence time is highest at the charged phosphate and carboxylate groups.

In the presence of Ca^{2+}, the residence times were drastically increased, thus emphasizing the importance of an electrostatic contribution to this increase. Moreover, this means that the positive charges of the cations are not shielded completely by the carboxylate and phosphate groups of the ReLPS. This is important for the assembly of aggregates of ReLPS held together by bivalent ions connecting the negatively charged ReLPS monomers by strong electrostatic intermolecular forces.

On the other hand, in the hydrophobic region, the coulombic interaction is weaker, but still the residence times are increased compared to bulk water. Sciortino et al. (1991) argued that a hydrophobic particle leads to a local dilution of the solvent, resulting in an increased stability of the hydrogen bond network, thus increasing residence times.

The diffusion coefficient of water, determined for those molecules that do not belong to the first hydration shell of the ReLPS molecules, is well within the range of values that can be found in the literature derived both from experimental and theoretical investigations (cf. Table 6). Thus, beyond the first hydration shell, bulk water-like diffusion rates were observed. Surprisingly, no influence of the presence of calcium cations on the water diffusion coefficient was found. Although water molecules from the first hydration shell were excluded from these calculations, from the increase of the mean residence times we expected an influence of the cations on the diffusion coefficient due to the long-range electrostatic forces underlying the attraction between the Ca^{2+} ions and the water molecules. Presumably, only a few water molecules were affected by these forces, whose effect was outnumbered by the large number of (bulk) water molecules unaffected by them, because of their greater distance from the cations.

The diffusion of the calcium ions was coupled to the motion of the ReLPS molecules through the strong electrostatic interaction between the positively charged ions and the negatively charged ReLPS molecules, thus resulting in a decreased net diffusion coefficient as compared to the "naked" Ca^{2+} ion. The diffusion coefficient of the ReLPS monomers was of the magnitude of 0.1×10^{-9} m^2/s. From the Stokes-Einstein relation, we calculated D(ReLPS) = 0.2×10^{-9} m^2/s, assuming that a ReLPS molecule can described as a spherical particle with a radius r = 15 Å, which is equivalent to half the maximum length of a ReLPS monomer (M_r = 2.2 kDa). The D value calculated this way is quite close to the result derived from the MD simulation. From ultracentrifugation experiments, Ribi et al. (1966) obtained $D = 0.03 \times 10^{-9}$ m^2/s for monomers of LPS with a molecular mass between 8.8 and 20.7 kDa, depending on the calculation method. The monomers were generated by the addition of a detergent. Taking into account the greater molecular mass of the LPS investigated by Ribi et al. and the uncertainty inherent in their results, the agreement between the experimental results and the values derived from the MD simulation is satisfactory.

TABLE 6 Diffusion coefficient D of water

Source	$D \pm$ SD w/ Ca^{2+} (10^{-9} m^2/s)	$D \pm$ SD w/o Ca^{2+} (10^{-9} m^2/s)
This work (simulation)	2.6 ± 0.2	2.6 ± 0.2
Sansom et al. (simul.)		3.2
Svishev and Kusalik (simul.)		2.2 ± 0.7
Weingärtner (exptl.)		2.3

This work: water molecules closer than 4 Å to the ReLPS molecules were excluded from the calculation of D.
Sansom et al. (1996): 231 TIP3P (modified), T = 300 K.
Svishev and Kusalik (1994): 256 SPC/E-water, T = 298 K.
Weingärtner (1982): experimental, T = 298.2 K.

CONCLUSION

The present paper is the first work describing the dynamic behavior of fully hydrated monomers of bacterial Re-lipopolysaccharide by means of molecular dynamics simulations. Six different conformations of *E. coli* ReLPS were simulated, in both the presence and absence of calcium ions. Our approach, which implied the parallel use of six different conformational models, enabled us to compare the behavior of the different models. This would have been impossible if we had conducted one extended simulation of one selected conformational model. The stabilization of most of the parameters investigated indicates that the investigated properties reached an equilibrium, which allows the evaluation of these data. Only the percentage of *gauche* defects did not reach equilibrium values during our limited simulation time, but from the literature the equilibration of this parameter is known to be very time consuming (Edholm and Nyberg, 1992).

Neither transition between nor convergence of the different starting structures was observed.

The calcium cations are strongly bound to the negatively charged headgroup of the ReLPS molecules, leading to a rigidification of the headgroup and a distortion of the GlcN backbone. The altered structure of the backbone influences the conformation of the linkage between the backbone and the fatty acids. As measured by the order parameter, in three of six cases, an increased mobility of the fatty acyl chains and a decreased order of the hydrophobic domain resulted as compared to simulations without bivalent cations. The conformation of the hydrophobic region of the ReLPS monomers showed a distinct flexibility, but the so-called micromembrane domain was always retained. From comparison to simulations carried out in vacuo, we deduced that this stability is induced by the presence of the solvent. The acyl chain order parameter is increased as compared to

model calculation for phospholipids, but the S_{CD} profile shows essentially the same structure. The high state of order and the small number of *gauche* defects of the fatty acid region of the ReLPS resemble those of the gel phase of phospholipids.

The solvent shell is strongly influenced by the hydrophobic and hydrophilic properties of the different regions of the ReLPS molecules. In the presence of Ca^{2+} ions, the mean residence time of water molecules is significantly increased in the headgroup region, implying an incomplete shielding of the positive charges of the cations, which is essential for the intermolecular "linkage" of aggregates by bivalent cations. Nevertheless, even in the hydrophobic region, the mean residence time of water molecules is significantly increased as compared to bulk water.

Becasue of the lack of experimental data, only a few parameters can be directly compared between our simulations and experiments; therefore the theoretical character of this work has to be stressed. But wherever possible, the validity of our simulation was confirmed. Moreover, data from the models investigated in this study were successfully used for the explanation of experimentally determined drug binding affinities of dicationic lipid A-binding molecules (David et al., 1995a). The efficient search for new drugs for the treatment of sepsis requires three-dimensional models of LPS, and we hope that the present work might stimulate the discussion on the structural requirements of potential high-affinity LPS-binding molecules by supplying a picture of LPS that is consistent with known experimental data.

The models used as starting structures of this investigation may represent the range of conformations *E. coli* ReLPS adopts in solution. Furthermore, they can be used to build aggregates of LPS that resemble the bacterial outer membrane and allow the investigation of drug-membrane interactions, e.g., with the antibiotic polymyxin b. From analysis of our data, we conclude that the starting structure best representing the average conformation of ReLPS molecules is conformation C.

Note

Sets of coordinates and charges of the starting structures are available from the corresponding author upon request.

The authors thank T. Gutberlet, P.-J. Koch, A. Sabisch, and W. Uebach for valuable discussions.

Financial support by the Deutsche Forschungsgemeinschaft is gratefully acknowledged.

REFERENCES

Allen, M. P., and D. J. Tildesley. 1987. Computer Simulation of Liquids. Oxford University Press, Oxford.

Alper, H. E., D. Bassolino-Klimas, and T. R. Stouch. 1993. The limiting behaviour of water hydrating a phospholipid monolayer: a computer simulation study. *J. Chem. Phys.* 99:5547–5559.

Appelmelk, B. J., A. Y. Qing, E. J. Helmerhorst, J. J. Maaskant, P. R. Abraham, L. G. Thijs, and D. M. MacLaren. 1995. Diversity in lipid A binding ligands: comparison of lipid A monoclonal antibodies with $rBPI_{23}$. *In* Bacterial Endotoxins: Lipopolysaccharides from Genes to Therapy. J. Levin, C. R. Alving, R. S. Munford, H. Redl, editors. Wiley-Liss, New York. 453–463.

Brade, H., L. Brade, and E. Th. Rietschel. 1988. Structure-activity relationships of bacterial lipopolysaccharides. *Zentralbl. Bakteriol. Mikrobiol. Hyg. A.* 268:151–179.

Brandenburg, K. 1993. Fourier transform infrared spectroscopy characterization of the lamellar and nonlamellar structures of free lipid A and Re lipopolysaccharide from *Salmonella minnesota* and *Escherichia coli*. *Biophys. J.* 64:1215–1231.

Brandenburg, K., H. Mayer, M. H. J. Koch, J. Weckesser, E. Th. Rietschel, and U. Seydel. 1993. Influence of the supramolecular structure of free lipid A on its biological activity. *Eur. J. Biochem.* 218:555–563.

Brooks, B. R., R. E. Bruccoleri, B. D. Olafson, D. J. States, S. Swaminathan, and M. Karplus. 1983. CHARMM: a program for macromolecular energy, minimization, and dynamics calculations. *J. Comput. Chem.* 4:187–217.

Brooks, C. L., and M. Karplus. 1989. Solvent effects on protein motion and protein effects on solvent motion. *J. Mol. Biol.* 208:159–181.

Brunne, R. M., E. Liepinsh, G. Otting, K. Wüthrich, and W. F. van Gunsteren. 1993. A comparison of experimental residence times of water molecules solvating the bovine pancreatic trypsin inhibitor with theoretical model calculations. *J. Mol. Biol.* 231:1040–1048.

Capodici, C., S. Chen, Z. Sidorczyk, P. Elsbach, and J. Weiss. 1994. Effect of lipopolysaccharide (LPS) chain length on interactions of bactericidal/permeability-increasing protein and its bioactive 23-kilodalton NH_2-terminal fragment with isolated LPS and intact *Proteus mirabilis* and *Escherichia coli*. *Infect. Immun.* 62:259–265.

Centers for Disease Control. 1990. Increase in national hospital discharge survey rates for septicemia—United States, 1979–1987. *MMWR. Morb. Mortal. Wkly. Rep.* 39:31–34.

Chiu, S.-W., M. Clark, V. Balaji, S. Subramaniam, H. L. Scott, and E. Jakobsson. 1995. Incorporation of surface tension into molecular dynamics simulation of an interface: a fluid phase lipid bilayer membrane. *Biophys. J.* 69:1230–1245.

Coughlin, R. T., A. Haug, and E. J. McGroarty. 1983a. Physical properties of defined lipopolysaccharide salts. *Biochemistry.* 22:2007–2013.

Coughlin, R. T., A. A. Peterson, A. Haug, H. J. Pownall, and E. J. McGroarty. 1985. A pH titration study on the ionic bridging within lipopolysaccharide aggregates. *Biochim. Biophys. Acta.* 821:404–412.

Coughlin, R. T., S. Tonsager, and E. J. McGroarty. 1983b. Quantitation of metal cations bound to membranes and extracted lipopolysaccharide of *Escherichia coli*. *Biochemistry.* 22:2002–2007.

David, S. A., P. Balaram, and V. I. Mathan. 1995b. Characterization of the interaction of lipid a and lipopolysaccharide with human serum albumin: implications for an endotoxin carrier function for albumin. *J. Endotoxin Res.* 2:99–106.

David, S. A., V. I. Mathan, and P. Balaram. 1995a. Interactions of linear dicationic molecules with lipid A: structural requisites for optimal binding affinity. *J. Endotoxin Res.* 2:325–336.

Din, Z. Z., P. Mukerjee, M. Kastowsky, and K. Takayama. 1993. Effect of pH on solubility and ionic state of lipopolysaccharide obtained from the deep rough mutant of *Escherichia coli*. *Biochemistry.* 32:4579–4586.

Doran, J. E. 1992. Biological effects of endotoxin. *Curr. Stud. Hematol. Blood Transfus.* 59:66–99.

Edholm, O., and A. M. Nyberg. 1992. Cholesterol in model membranes. *Biophys. J.* 63:1081–1089.

Gally, H. U., G. Pluschke, P. Overath, and J. Seelig. 1979. Structure of *Escherichia coli* membranes. Phospolipid conformation in model membranes and cells as studied by deuterium magnetic resonance. *Biochemistry.* 18:5605–5610.

Gally, H. U., G. Pluschke, P. Overath, and J. Seelig. 1980. Structure of *Escherichia coli* membranes. Fatty acyl chain order parameters of inner and outer membranes and derived liposomes. *Biochemistry.* 19: 1638–1643.

Garcia, A. E., and L. Stiller. 1993. Computation of the mean residence time of water in the hydration shells of biomolecules. *J. Comput. Chem.* 14:1396–1406.

Gray, P. W., G. Flaggs, S. R. Leong, R. J. Gumina, J. Weiss, C. Eng Oi, and P. Elsbach. 1989. Cloning of the cDNA of a human neutrophil bactericidal protein. Structural and functional correlations. *J. Biol. Chem.* 264:9505–9509.

Gutberlet, T. 1989. Kraftfeldrechnungen zum Einfluß intramolekularer elektrostatischer Wechselwirkungen auf Konformationen von Re-Lipopolysaccharid von *Escherichia coli*. Diplomarbeit, Freie Universität Berlin, Berlin, Germany.

Hagler, A. T., and J. Moult. 1978. Computer simulation of the solvent structure around biological macromolecules. *Nature.* 272:222–226.

Hauser, H. 1973. Lipids. *In* Water: A Comprehensive Treatise, Vol. 4: Aqueous Solutions of Amphiphiles and Macromolecules. F. Franks, editor. Plenum Press, New York. 209–303.

Helander I. M., P. H. Mäkelä, O. Westphal, and E. Th. Rietschel. 1995. Lipopolysaccharides. *In* Molecular Biology and Biotechnology. R. A. Meyers, editor. VCH, Weinheim. 509–511.

Holst, O., W. Broer, J. E. Thomas-Oates, U. Mamat, and H. Brade. 1993. Structural analysis of two oligosaccharide bisphosphates from the lipopolysaccharide of a recombinant strain of *Escherichia coli* F515 (Re chemotype) expressing the genus-specific epitope of *Chlamydia* lipopolysaccharide. *Eur. J. Biochem.* 214:703–710.

Imoto, M., S. Kusumoto, T. Shiba, E. Th. Rietschel, C. Galanos, and O. Lüderitz. 1985a. Chemical structure of *Escherichia coli* lipid A. *Tetrahedron Lett.* 26:907–908.

Imoto, M., H. Yoshimura, N. Sakaguchi, S. Kusumoto, and T. Shiba. 1985b. Total synthesis of *Escherichia coli* lipid A. *Tetrahedron Lett.* 26:1545–1548.

Impey, R. W., P. A. Madden, and I. R. McDonald. 1983. Hydration and mobility of ions in solution. *J. Phys. Chem.* 87:5071–5083.

Israelachvili, J. N., S. Marcelja, and R. G. Horn. 1980. Physical principles of membrane organization. *Q. Rev. Biophys.* 13:121–200.

Jorgensen, W. L., J. Chandrashekar, J. D. Madura, R. W. Impey, and M. L. Klein. 1983. Comparison of simple potential functions for simulating liquid water. *J. Chem. Phys.* 79:926–935.

Jung, S., D. Min, and R. I. Hollingsworth. 1996. A metropolis Monte Carlo method for analyzing the energetics and dynamics of lipopolysaccharide supramolecular structure and organization. *J. Comput. Chem.* 17: 238–249.

Kaca, W., R. I. Roth, and J. Levin. 1994. Hemoglobin, a newly recognized lipopolysaccharide (LPS)-binding protein that enhances LPS biological activity. *J. Biol. Chem.* 269:25078–25084.

Karplus, M., and G. A. Petsko. 1990. Molecular dynamics simulations in biology. *Nature.* 347:631–639.

Kastowsky, M. 1993. Modelling the three-dimensional structure of lipopolysaccharide. *In* Bacterial Endotoxin: Recognition and Effector Mechanisms. J. Levin, C. R. Alving, R. S. Munford, and P. L. Stütz, editors. Elsevier, Amsterdam. 61–70.

Kastowsky, M., T. Gutberlet, and H. Bradaczek. 1992. Molecular modelling of the three-dimensional structure and conformational flexibility of bacterial lipopolysaccharide. *J. Bacteriol.* 174:4798–4806.

Kastowsky, M., T. Gutberlet, and H. Bradaczek. 1993. Comparison of x-ray powder-diffraction data of various bacterial lipopolysaccharide structures with theoretical model conformations. *Eur. J. Biochem.* 217: 771–779.

Kastowsky, M., A. Sabisch, and H. Bradaczek. 1991a. MEMBRANE: a program for simulation and analysis of x-ray diffraction patterns of thin multilayer films. *Makromol. Chem. Macromol. Symp.* 46:187–191.

Kastowsky, M., A. Sabisch, T. Gutberlet, and H. Bradaczek. 1991b. Molecular modelling of bacterial deep rough mutant lipopolysaccharide of *Escherichia coli*. *Eur. J. Biochem.* 197:707–716.

Kato, N., M. Ohta, N. Kido, Y. Arakawa, T. Sugiyama, S. Naito, and H. Ito. 1993. Polymorphism of crystals of *Salmonella minnesota* Re and Ra lipopolysaccharides. *Microbiol. Immunol.* 37:549–555.

Kirikae, T., F. U. Schade, U. Zähringer, F. Kirikae, H. Brade, S. Kusumoto, T. Kusama, and E. Th. Rietschel. 1994. The significance of the hydrophilic backbone and the hydrophobic fatty acid regions of lipid A for macrophage binding and cytokine induction. *FEMS Immunol. Med. Microbiol.* 8:13–26.

Labischinski, H., G. Barnickel, H. Bradaczek, D. Naumann, E. Th. Rietschel, and P. Giesbrecht. 1985. High state of order of isolated bacterial lipopolysaccharide and its possible contribution to the permeation barrier property of the outer membrane. *J. Bacteriol.* 162:9–20.

Labischinski, H., E. Vorgel, W. Uebach, R. P. May, and H. Bradaczek. 1990. Architecture of bacterial lipid A in solution. A neutron small-angle scattering study. *Eur. J. Biochem.* 190:359–363.

Leroux, B., H. Bizot, J. W. Brady, and V. Tran. 1995. Anisotropic water distribution around α-D-glucose by molecular dynamics simulation. Second Symposium on Biological Physics, Munich. 47.

Martich, G. D., A. J. Boujoukos, and A. F. Suffredini. 1993. Response of man to endotoxin. *Immunobiology.* 187:403–416.

Mattsby-Baltzer, I., K. Lindgren, B. Lindholm, and L. Edebo. 1991. Endotoxin shedding by enterobacteria: free and cell-bound endotoxin differ in *Limulus* activity. *Infect. Immun.* 59:689–695.

Mendelsohn, R., M. A. Davies, W. Brauner, H. F. Schuster, and R. A. Dluhy. 1989. Quantitative determination of conformational disorder in the acyl chains of phospholipid bilayers by infrared spectroscopy. *Biochemistry.* 28:8934–8939.

Morrison, D. C. 1989. The case for specific lipopolysaccharide receptors expressed on mammalian cells. *Microb. Pathog.* 7:389–398.

Nichol, C. P., J. H. Davis, G. Weeks, and M. Bloom. 1980. Quantitative study of the fluidity of *Escherichia coli* membranes using deuterium magnetic resonance. *Biochemistry.* 19:451–457.

Nikaido, H., and M. Vaara. 1987. Outer membrane in *Escherichia coli* and *Salmonella typhimurium*. *In* Cellular and Molecular biology. C. Neidhardt, J. L. Ingraham, K. Brooks Low, B. Magasanik, M. Schaechter, and H. E. Umbarger, editors. American Society for Microbiology, Washington, DC. 7–22.

Obst, S., and H. Bradaczek. 1996. Molecular dynamics study of the structure and dynamics of the hydration shell of alkaline and alkaline-earth metal cations. *J. Phys. Chem.* 100:15677–15687.

Otting, G., E. Liepinsh, and K. Wüthrich. 1991. Protein hydration in aqueous solution. *Science.* 254:974–980.

Pelletier, C., P. Bourlioux, and J. van Heijenoort. 1994. Effects of subminimal inhibitory concentrations of EDTA on growth of *Escherichia coli* and the release of lipopolysaccharide. *FEMS Microbiol. Lett.* 117: 203–206.

Raetz, C. R. H. 1990. Biochemistry of endotoxins. *Annu. Rev. Biochem.* 59:129–170.

Raetz, C. R. H., R. J. Ulevitch, S. D. Wright, C. H. Sibley, A. Ding, and C. F. Nathan. 1991. Gram-negative endotoxin: an extraordinary lipid with profound effects on eukaryotic signal transduction. *FASEB J.* 5:2652–2660.

Ribi, E., L. Anacker, R. Brown, W. T. Haskins, B. Malmgren, K. C. Milner, and J. A. Rudbach. 1966. Reaction of endotoxin and surfactants. *J. Bacteriol.* 92:1493–1509.

Rietschel, E. Th., and H. Brade. 1992. Bacterial endotoxins. *Sci. Am.* 267:26–33.

Rietschel, E. Th., T. Kirikae, F. U. Schade, U. Mamat, G. Schmidt, H. Loppnow, A. J. Ulmer, U. Zähringer, U. Seydel, F. Di Padova, M. Schreier, and H. Brade. 1994. Bacterial endotoxin: molecular relationships of structure to activity and function. *FASEB J.* 8:217–225.

Rietschel, E. Th., T. Kirikae, F. U. Schade, A. J. Ulmer, O. Holst, H. Brade, G. Schmidt, U. Mamat, H.-D. Grimmecke, S. Kusumoto, and U. Zähringer. 1993. The chemical structure of bacterial endotoxin in relation to bioactivity. *Immunobiology.* 187:169–190.

Rietschel, E. Th., H. Mayer, H.-W. Wollenweber, U. Zähringer, O. Lüderitz, O. Westphal, and H. Brade. 1984. Bacterial lipopolysaccharides and their lipid A component. *In* Bacterial Endotoxin: Chemical, Biological and Clinical Aspects. J. Y. Homma, editor. Verlag Chemie, Basel. 11–22.

Risco, C., and P. Pinto da Silva. 1995. Cellular functions during activation and damage by pathogens: immunogold studies of the interaction of bacterial endotoxins with target cells. *Microsc. Res. Tech.* 31:141–158.

Sabisch, A. 1994. Verbindung von eindimensionalen Röntgendaten an lamellaren Schichten mit modelling-Experimenten am Beispiel von bakteriellen Lipopolysacchariden. Thesis. Freie Universität Berlin, Berlin, Germany.

Sansom, M. S. P., I. D. Kerr, J. Breed, and S. Sankararamakrishnan. 1996. Water in channel-like cavities: structure and dynamics. *Biophys. J.* 70:693–702.

Schumann, R. R., S. R. Leong, G. W. Flaggs, P. W. Gray, S. D. Wright, J. C. Mathison, P. S. Tobias, and R. J. Ulevitch. 1990. Structure and function of lipopolysaccharide binding protein. *Science.* 249: 1429–1431.

Sciortino, F., A. Geiger, and E. H. Stanley. 1991. Effects of defects on molecular mobility in liquid water. *Nature.* 354:218–221.

Seddon, J. M., G. Cevc, and D. Marsh. 1983. Calorimetric studies of the gel-fluid (L_β-L_α) and lamellar-inverted hexagonal (L_α-H_{II}) phase transition in dialkyl- and diacylphosphatidylethanolamines. *Biochemistry.* 22:1280–1289.

Seelig, J., and A. Seelig. 1974. The dynamic structure of fatty acyl chains in a phospholipid bilayer measured by deuterium magnetic resonance. *Biochemistry.* 13:4839–4845.

Seydel, U., H. Labischinski, M. Kastowsky, and K. Brandenburg. 1993. Phase behaviour, supramolecular structure, and molecular conformation of lipopolysaccharide. *Immunobiology.* 187:191–211.

Shnyra, A., K. Hultenby, and A. A. Lindberg. 1993. Role of the physical state of *Salmonella* lipopolysaccharide in expression of biological and endotoxic properties. *Infect. Immun.* 61:5351–5360.

Svishchev, I. M., and P. G. Kusalik. 1994. Dynamics in liquid H_2O, D_2O, and T_2O: a comparative simulation study. *J. Phys. Chem.* 98:728–733.

Takayama, K., Z. Z. Din, P. Mukerjee, P. H. Cooke, and T. N. Kirkland. 1990. Physicochemical properties of the lipopolysaccharide unit that activates B lymphocytes. *J. Biol. Chem.* 265:14023–14029.

Takayama, K., D. H. Mitchell, Z. Z. Din, P. Mukerjee, C. Li, and D. L. Coleman. 1994. Monomeric Re lipopolysaccharide from *Escherichia coli* is more active than the aggregated form in the *Limulus* amebocyte lysate assay and in inducing Egr-1 mRNA in murine peritoneal macrophages. *J. Biol. Chem.* 269:2241–2244.

Tanford, C. 1972. Micelle shape and size. *J. Phys. Chem.* 76:3020–3024.

Tobias, P. S., K. Soldau, and R. J. Ulevitch. 1989. Identification of a lipid A binding site in the acute phase reactant lipopolysaccharide binding protein. *J. Biol. Chem.* 264:10867–10871.

Vaara, M. 1992. Agents that increase the permeability of the outer membrane. *Microbiol. Rev.* 56:395–411.

van Gunsteren, W. F., and H. J. C. Berendsen. 1977. Algorithms for macromolecular dynamics and constraint dynamics. *Mol. Phys.* 34: 1311–1327.

van Gunsteren, W. F., and H. J. C. Berendsen. 1990. Molecular dynamics computer simulation. Method, application and perspectives in chemistry. *Angew. Chem. Int. Ed. Engl.* 29:992–1027.

Weingärtner, H. 1982. Self diffusion in liquid water. A reassessment. *Z. Phys. Chem. NF.* 132:129–149.

Wright, S. D., R. A. Ramos, P. S. Tobias, R. J. Ulevitch, and J. C. Mathison. 1990. CD14, a receptor for complexes of lipopolysaccharide (LPS) and LPS binding protein. *Science.* 249:1431–1433.

Zähringer, U., B. Lindner, and E. Th. Rietschel. 1994. Molecular structure of lipid A, the endotoxic center of bacterial lipopolysaccharides. *Adv. Carbohydr. Chem. Biochem.* 50:211–76.

Zähringer, U., B. Lindner, U. Seydel, E. Th. Rietschel, H. Naoki, F. M. Unger, M. Imoto, S. Kusumoto, and T. Shiba. 1985. Structure of De-O-acylated lipopolysaccharide from the *Escherichia coli* Re mutant strain F515. *Tetrahedron Lett.* 26:6321–6324.